Fermilab
ES&H Section

R. P. Note No. 125

A STUDY OF NEUTRON ROOM SCATTERING AT RPCF

October 22, 1996

Written By: Andrew C. Kemp

Written By: Dave Boehnlein

Written By: Alex Elwyn

Written By: Kamran Vaziri

Reviewed By: Don Cossairt, Associate Head for Radiation Protection — 10/29/96 Date

Reviewed By: Bill Griffing, ES&H Section Head — 10/30/96 Date

Distribution via QuickMail
Radiation Protection Group

RADIATION PHYSICS NOTE 125

A STUDY OF NEUTRON ROOM SCATTERING AT RPCF

Andrew Kemp, David Boehnlein, Alex Elwyn, and
Kamran Vaziri

AUGUST 1996

I. *INTRODUCTION*

High energy physics facilities must monitor the radiation doses received by their personnel. This monitoring can only be effective if the radiation detection devices can be calibrated with a good degree of accuracy. Radiation fields are usually composed of several types of radiation, including gamma rays, beta radiation, neutrons, etc. A complication arises during calibration of neutron detection instruments because they respond not only to the neutrons coming directly from the source but also those scattered from the floor, walls, and ceiling. The amount of neutron scattering varies from site to site depending on the construction materials and layout of the building. The purpose of this study was to determine the scattered neutron fraction in the central volume of the calibration mezzanine of the Radiation Physics Calibration Facility at site 38 (RPCF) at the Fermi National Accelerator Laboratory (Fermilab).

At Fermilab, radiation workers wear dosimeters that use CR39 for neutron detection. The badges are sent to an outside vendor for reading. As part of the quality assurance program, Fermilab routinely sends the vendor "spiked" badges, i.e. CR39s exposed to a neutron source of known strength for a given amount of time at a fixed distance on the mezzanine in the RPCF. The dose received by CR39s during spiking is a mixture of neutrons coming directly from the source and those scattered from the material of the room. This study is important, then, because the dose deposited on the badges by scattered neutrons during the spiking runs was not previously known.

The study was conducted in a room with floor dimensions of 12 m by 9.5 m. The walls and ceiling are thin steel and insulation supported by steel I-beams. It is likely that neutrons scattered from the concrete floor dominate the scattered portion of neutrons in the RPCF. We determined the total amount of radiation at 3 heights above the floor, and at three distances from an AmBe neutron source at each height in the RPCF using the Bonner Sphere (multisphere) technique (see Awschalom and Sanna 1983). We determined the scattered fractions of the total fluence by three methods: subtraction of an ideal direct value from the total measured fluence, a curve-fitting technique, and a formula from Jenkins (1980) which represents a simple recipe for scattering from the ground or a concrete surface. Equations for total fluence and dose equivalent by Jenkins (1980) were found to fit our measured values at each height to within about 10%, implying that the amount of neutron scattering can now be predicted for almost any configuration of source and detector in the RPCF.

II. EQUIPMENT

Detectors were exposed to an ^{241}AmBe source (Fermilab source identification number: 241Be-7.2-1) having a flux of 1.98×10^7 neutrons per second (Krueger 1992). This is the same source used for most spiking runs of badges because its spectrum resembles that found outside radiation shields at Fermilab. The source was covered by a lead cap about 4 mm thick to remove the large number of 59.6 keV gamma rays from ^{241}Am decay. Neutrons were moderated by a set of polyethylene Bonner spheres, each containing its own 12.7 mm high x 12.7 mm diameter ^{6}LiI(Eu) scintillation detector. The detection of neutrons is based on the exothermic ^{6}Li(n,α)^{3}H thermal capture reaction (Q-value = 4.78 MeV, $\sigma_{n,\alpha}$ = 940 barns). The spheres had the following diameters: 5.08 cm, 7.62 cm, 12.7 cm, 20.32 cm, 25.4 cm, 30.48 cm, and 45.72 cm. One unmoderated (bare) detector was also used in each test. Spheres were placed on an aluminum scaffold propped between two aluminum ladders (Figure 1).

The Bonner Spheres were placed one at a time into the neutron field of the source. The signal from each photomultiplier was transmitted through an amplifier to a multiplex router (M/R) and an ADC, and finally into a PC based data acquisition system (Figure 2; see Cossairt, et al. 1988 for more details). Software developed by Canberra, called the System 100 (S100), allowed the use of the computer as a multichannel analyzer. A count rate for each run was obtained from the spectrum by marking the boundary of the peak of interest. The S100 automatically fit a background and extracted the area of the peak above background. (See the Appendix for a short discussion of data analysis from an AmBe source.)

III. METHODS

The source and detectors were placed at the same heights above the floor for any given run. The three heights used were 37.5 cm, 94.8 cm, and 239.2 cm. The spheres were also placed at three distances from the source for each height: 100 cm, 150 cm, and 200 cm. Heights and distances were measured with respect to the geometrical centers of the source and spheres.

Detectors were exposed one at a time in order to avoid potential problems with nonuniformities in the radiation field, and the possibility of sphere to sphere "crosstalk." Detectors were exposed for a time sufficient to register a minimum of 10,000 counts. Thus, the 5.08 cm sphere was exposed for 45 minutes, exposures of the bare detector were made for 100 minutes, and the remaining spheres were given 10 minute exposures.

The possibility existed that the room may not scatter neutrons uniformly. To test this possibility, the source was placed at a height of 37.5 cm at the exact center of the floor area in the mezzanine, and the 12.7 cm sphere was placed at distances of 1 m and 2 m towards each side of the room (Figures 3a and 3b). The source was also moved 1 m from room center (Figures 4a and 4b). The radiation field appeared uniform for this detector at this height.

The counts registered by the 12.7 cm sphere were compared when the source stand was on and off a wooden cart normally used during the spiking runs. There was a 3% to 4% increase in count rate when the wooden cart was used at the 37.5 cm height, and essentially no change within the errors at a height of 181.5 cm (Figures 5 a - d). Nonetheless, the cart was not used in this experiment.

The neutron fluence spectrum was unfolded from individual sphere responses using the computer program BUNKI (see Elwyn 1989 and references therein for a discussion of unfolding spectra from measured multisphere counting rates). This program calculates the total measured fluence (F_m) in units of N/cm^2/min, as well as several other quantities of interest, such as dose equivalent. The response matrices of Sanna (see Awschalom and Sanna 1983) were used in these calculations. It is assumed that these sphere efficiencies represent the true energy dependence of the detectors.

There are several possible routes to determine the amount of neutron scattering, each with its advantages and disadvantages. Here, we use 3 methods, discussed below.

Method 1: Subtraction

If total measured fluence (F_m) is the sum of those neutrons detected as coming directly at the detector (F_D) and those neutrons scattered into the detector (F_S), then

$$F_S = F_m - F_D, \tag{1}$$

The scattered fraction (S_S), then, is F_S/F_m.

F_D can be determined theoretically by assuming that the neutron radiation arises from a point-like isotropic source, and follows the inverse-square law. Thus, the ideal direct fluence (F_D) at a given point can be predicted from

$$F_D = Q \Big/ 4\pi r_0^2, \tag{2}$$

where Q is the source neutron rate, and r_o is the source to detector distance.

Substituting equation 2 in equation 1 requires the assumption that there is no difference between the actual and theoretical direct fluence, an unlikely situation. Differences between the ideal and actual direct fluence can arise from the anisotropy of the source, air scattering (Eisenhauer, et al. 1982), and small finite errors in the measurement of source-to-detector distance. Nevertheless, experience suggests equation 2 is a reasonable approximation of F_D

Method 2: Curve-fitting

The observed total response for each sphere—on the assumption that air scattering, source anisotropy, and geometric corrections are negligible—is given by

$$C_{obs} = a \Big/ {r_0}^2 + b, \tag{3}$$

where r_0 is the source to detector distance, a/r_0^2 is the direct neutron contribution from the source, and b, the room scattering contribution, is assumed to be independent of distance from the source. This should be a good assumption if both source and detector are placed at large heights above the floor. The coefficients a and b were obtained for each detector at each height by fitting equation 3 to a plot of count rate versus r_0(Figure 6). The direct and scattered count rates from the fit for all spheres at each height were entered into the BUNKI program to obtain fluences and dose equivalents for the direct and scattered portions separately. The scattered fluence portion divided by the total measured fluence (F_m), which will be different at each distance r_0 from the source, give the scattered fractions (S_C) for this method.

Method 3: Jenkins' formulas.

Using a wide range of energies and source to detector configurations, Jenkins (1980) has determined an empirical formula for predicting the fluence due to neutrons scattered mainly from one surface (F_1). His formula is based on a simple geometric model and may be written as:

$$F_1 = F_D N \qquad (4)$$

where F_D is, again, the "ideal" fluence calculated from equation (2), and N is the fluence scattering factor determined from

$$N = \frac{1.52\, R/r_0}{(1+0.1E)\left[1+(R/r_0)^3\right]}, \qquad (5a)$$

where R is the total distance traveled by the neutrons, from the source to the detector, after one bounce from the floor, in the same units as r_0 and E is the average energy (in MeV) of the neutrons from the source, which for an ^{241}AmBe source is assumed to be 4.2 MeV. Therefore, for the AmBe source equation (5a) reduces to

$$N = \frac{1.07\, R/r_0}{1+(R/r_0)^3} \qquad (5b)$$

Jenkins' (1980) formula for total fluence can be written as

$$F_J = F_D + F_1 \qquad (6)$$

Therefore the scattered fluence fraction (S_J) is F_1/F_J.

IV. RESULTS & DISCUSSION

The scattered fractions determined by the three methods are shown in Table 1. The largest differences are found at the lowest height.

Specifically, the amount of scattering found at h = 37.5 cm by the curve-fitting method is significantly less than the scattering predicted by the other two methods at this height.

The direct neutron contribution to the measured fluence is proportional to $1/r_0^2$, but the scattered portion is not so constrained. Therefore, we expected the contribution of scattered neutrons to the total fluence to become proportionally larger as the source-to-detector distance increased. This hypothesis is supported by the results of all three methods used for determining scattered fractions (Table 1).

Neutrons may be scattered by any atoms they encounter, but they are scattered best by materials with high hydrogen content, such as concrete (Cember 1989). We expect that the higher the detectors were above the concrete floor, the lower the number of scattered neutrons they would intercept. Except for the scattered fraction at h=37.5 cm determined from curve-fitting, the scattered neutron fractions shown in Table 1 are inversely proportional to height, supporting this hypothesis.

In the curve-fitting method, there is a smaller percentage of scattered neutrons near the floor than there are at the larger heights, a result which contradicts expectations from geometric considerations, as well as differing from the results of the other two methods for calculating scattering. It should be recalled that the curve-fitting method assumes that the amount of scattering is independent of distance from the source. At a height of only 37.5 cm from a thick scatterer (the floor) this assumption is clearly not satisfied. Equation 3 is not a good approximation at this height. It appears in fact from a comparison with the results from the Jenkins' formula, that based on the present study equation 3 represents a good approximation to determine room scattering only for source and detector at heights greater than 200 cm above the floor.

Ideally, we would like to have an equation which can predict the total fluence, including the scattered portion, for any height and distance in the RPCF. The formula (equation 6) given by Jenkins (1980) provides such an opportunity. The fluence values actually measured in the RPCF agree to within 10% with those predicted by equation 6 (Table 2). Therefore, total fluences within 10% of those measured in the RPCF can be calculated using

$$F_{tot} = (F_D + F_1). \qquad (7)$$

Jenkins (1980) also derived a corresponding formula for the dose equivalent of the scattered fraction ($D.E._{scat}$) which can be written,

$$D.E._{scat} = CF_D f \qquad (8)$$

The variable "C" is the source fluence-to-dose conversion factor; for our source C has a value of 0.137 (mrem/hr)/(n/cm^2•sec) (Krueger 1992). The variable f is the dose equivalent scattering factor. This factor may be calculated from

$$f = \frac{0.75\, R/r_0}{1 + \left(R/r_0\right)^3} \qquad (9)$$

The scattered contribution to the dose equivalent calculated from the curve fitting method is given in Table 3. It should be noted that dose-equivalent due to scattered neutrons should be the same at all source to detector distances by use of this method. At the lower height, the calculated values are not very close to those predicted by the Jenkins equation (Table 4) because of the limitations on use of equation 3 at these heights, as discussed earlier. However, the total dose equivalents predicted by Jenkins' formula are close to those determined in this study, as obtained from actual measured counting rates by use of BUNKI. Jenkins' formula for total dose equivalent may be written as

$$D.E._J = (F_D C)(1 + f). \qquad (10)$$

On the average equation 10 gives values about 9% higher than those measured (Table 5).

Using the scattered and direct fractions obtained at the 239 cm height from the curve fitting method, the count rates obtained for each sphere at each distance were separated into the direct and scattered portions. These direct and scattered count rates were input into BUNKI to produce their respective neutron spectra. Figure 7 shows a typical plot of fluence (n/cm^2-min) per unit lethargy as a function of neutron energy for the scattered and the direct neutrons. The scattered neutrons are more than an order of magnitude less intense than the direct neutrons, and the peak energy is about an order of magnitude lower than that of the direct neutrons.

V. CONCLUSIONS

There is a significant amount of neutron scattering in the RPCF, mostly arising from the concrete floor. Spiking runs are usually conducted at a height of about 2 meters and a horizontal distance of 1 meter. The data from this study suggest scattered neutrons contribute about 15% to 20% to the total fluence and 10% to the dose-equivalent at this configuration. The contribution of scattering to total fluence can now be predicted by using the formula, $F_{tot} = (F_D + F_I)$, with F_I given by equation 4. The dose equivalent can also be calculated using the formula, $D.E._{tot} = (F_D C)(1 + f)$.

Although the present study detailing the fractions and energy spectra associated with scattered neutrons at RPCF only holds rigorously for moderated spherical neutron detectors, the fact that the measurements agree with the formulae for the scattered fraction given by Jenkins (which are independent of the particular neutron detection technique) gives confidence that the results should hold for any detector used during spiking activities.

We were also able to show the following:

- at 37.5 cm high, the neutron field with this source in the RPCF is uniform enough to allow the source to be moved up to 1 meter away from floor center without affecting the flux measured by the 12.7 cm sphere;
- at 37.5 cm high, the flux measured with respect to each wall by the 12.7 cm sphere is relatively uniform up to 200 cm from floor center, so exposures can be made in any given direction without changing the results;
- the wooden cart which is part of the usual set-up to "spike" badges contributes about 3% of the neutrons detected by the 12.7 cm Bonner sphere at a height of 37.5 cm. At 200 cm height, where spiking is done, this effect is negligible.

Acknowledgments—Financial support for this project was partially provided by the Teacher Research Associate (TRAC) Program, which is administered by Associated Western Universities, Inc., and sponsored by the U. S. Department of Energy.

VI. REFERENCES

Awschalom, M.; Sanna, R. S. Applications of Bonner sphere detectors in neutron field dosimetry. Fermilab TM-1209, 1183.000; 1983. (Also Radiat. Prot. and Dosim. 10: 89-101; 1985.)

Cember, H. Introduction to Health Physics, 2nd ed.; New York: Pergamon Press: 127; 1989

Cossairt, J. D.; Elwyn, A.J.; Freeman, W.S.; Salsbury, W.C.; Yurista, P. M. Measurements of neutrons in enclosures and outside of shielding at the Tevatron. Proceedings of the 22nd Midyear Tropical Meeting of the Health Physics Society. San Antonio, Texas; Dec. 4 - 8, 1988.

Eisenhauer, C. M.; Schwartz, R. B.; McCall, R. C. Effect of air scatter on calibration of instruments for detecting neutrons. Radiat. Prot. Dosim. 19: 77-84; 1987.

Elwyn, A. Observations on spectrum unfolding with BUNKI. Fermilab Radiation Physics Note 80; 1989.

Jenkins, T. M. Simple recipes for ground scattering in neutron detector calibration. Health Phys. 39: 41-47; 1980.

Krueger, F. Calibration of radioactive sources used by Fermilab ES&H Section for instrument calibration and characterization. Fermilab Radiation Physics Note 83; 1992.

Appendix:

Notes on Analysis of Data from use of an AmBe Source

One of the experimental problems associated with the determination of the counting rate for the bare detector, and to a lesser extent with the 5.08 cm detector as well, is the fact that there are so few low energy neutrons emitted by the AmBe source. One observed, in fact, the existence of two peaks on the measured pulse height spectrum. The first peak represents the standard peak that arises from thermal neutron detection. The second one seems to be associated with the detection of neutrons with energies of around 250 keV, at which energy there is a resonance in the Li total neutron cross section. This peak is clearly visible in the energy dependence of the calculated response function (see Awschalom and Sanna,1983) for the bare sphere, although not for the 5.08 cm sphere. For the bare detector this second peak represents as much as about 40% of the total contribution (but at least 22%) if both peaks are selected as the "true" detected neutrons. (For the 5.08 cm sphere, this contribution is generally less than about 14%, with an average of about 6%. The effect is thus much less important in the determination of the counting rate than with the bare detector). While there is some uncertainty about whether the 2nd peak should actually be included in the data analysis, or whether only the first ("thermal") peak should be used, the gross properties of the neutron spectrum from the AmBe source are hardly affected one way or the other.

To illustrate this last point, Fig. A1 shows the measured direct AmBe spectrum (in units of lethargy, or log energy) unfolded by BUNKI for a number of different assumptions concerning the contribution from the bare and 5.08 cm sphere. As can be seen the spectrum is very closely the same whether one or two peaks are taken for the bare and 5.08 cm diameter spheres, or indeed even when no bare detector is used in the unfolding process. Furthermore, the values of total fluence determined by BUNKI for the three cases shown here differ by less than 5%, and dose-equivalent by 1% at the most.

Table 1: Comparison of scattered fractions determined by 3 methods: S_S = subtraction method, S_C = curve-fitting method, and S_J = Jenkins formula (equation 3).

Table 1a: Source to detector distance = 100 cm.

	S_S	S_C	S_J
h=239.2 cm	14.9 %	3.6 %	4.3 %
h=94.8 cm	21.9 %	8.5 %	17.4 %
h=37.5 cm	37.0 %	1.5 %	31.2 %

Table 1b: Source to detector distance = 150 cm.

	S_S	S_C	S_J
h=239.2 cm	18.6 %	7.7 %	8.5 %
h=94.8 cm	30.1 %	17.1 %	25.0 %
h=37.5 cm	38.3 %	3.2 %	33.3 %

Table 1c: Source to detector distance = 200 cm.

	S_S	S_C	S_J
h=239.2 cm	23.5 %	12.9 %	13.0 %
h=94.8 cm	37.4 %	27.3 %	29.1 %
h=37.5 cm	39.0 %	5.7 %	34.0 %

Table 2: Total measured fluences (F_m) compared to those predicted by the Jenkins formula (F_J).

Table 2a: Source to detector distance = 100 cm.

	F_m ($N/cm^2/min$)	F_J ($N/cm^2/min$)
h=239.2 cm	11110	9875
h=94.8 cm	12100	11439
h=37.5 cm	15010	13736

Table 2b: Source to detector distance = 150 cm.

	F_m ($N/cm^2/min.$)	F_J ($N/cm^2/min.$)
h=239.2 cm	5164	4592
h=94.8 cm	6008	5601
h=37.5 cm	6807	6298

Table 2c: Source to detector distance = 200 cm.

	F_m ($N/cm^2/min.$)	F_J ($N/cm^2/min.$)
h=239.2 cm	3087	2718
h=94.8 cm	3773	3332
h=37.5 cm	3872	3581

Table 3: Scattered neutron contribution to dose equivalent as determined by the curve-fitting method. Values are from the BUNKI program.

Height (cm)	Dose equivalent (mrem/hr).
239.2	0.614
94.8	1.673
37.5	0.496

Table 4: Predicted scattered neutron contribution to dose equivalent (D.E.$_{scat}$, in mrem/hr) as determined by Jenkins' (1980) formula.

	r=100 cm	r=150 cm	r=200 cm
h=239.2 cm	0.822	0.766	0.691
h=94.8 cm	3.910	2.730	1.877
h=37.5 cm	8.353	4.090	2.375

Table 5: Comparison of measured dose equivalent($D.E._m$) and dose equivalent predicted by Jenkins' formula ($D.E._J$).

Table 5a: Source to detector distance = 100 cm.

	$D.E._m$ (mrem/hr)	$D.E._J$ (mrem/hr)
h=239.2 cm	25.90	27.13
h=94.8 cm	25.33	30.22
h=37.5 cm	30.82	34.67

Table 5b: Source to detector distance = 150 cm.

	$D.E._m$ (mrem/hr)	$D.E._J$ (mrem/hr)
h=239.2 cm	11.94	12.46
h=94.8 cm	12.68	14.42
h=37.5 cm	14.04	15.78

Table 5c: Source to detector distance = 200 cm.

	$D.E._m$ (mrem/hr)	$D.E._J$ (mrem/hr)
h=239.2 cm	6.972	7.269
h=94.8 cm	7.686	8.455
h=37.5 cm	7.962	8.954

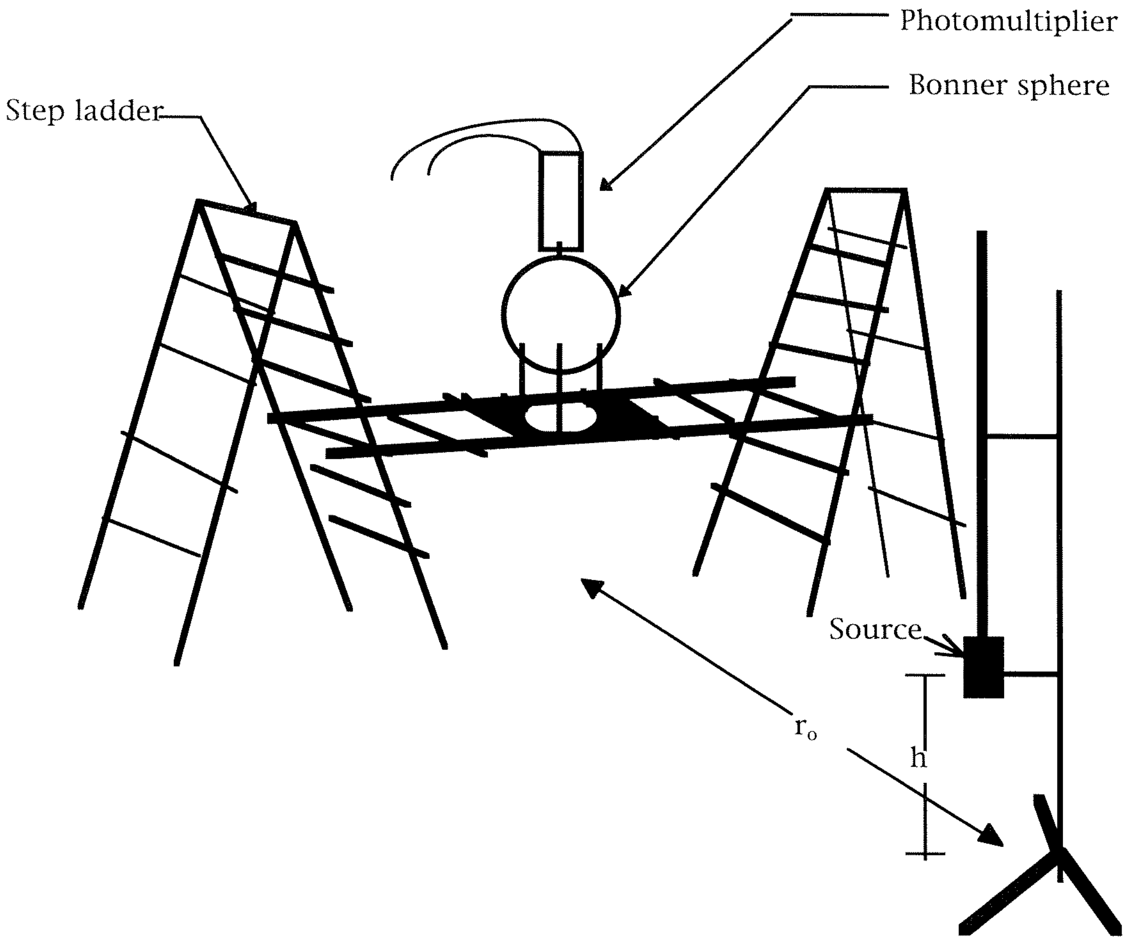

Figure 1. A diagram of the experimental setup.

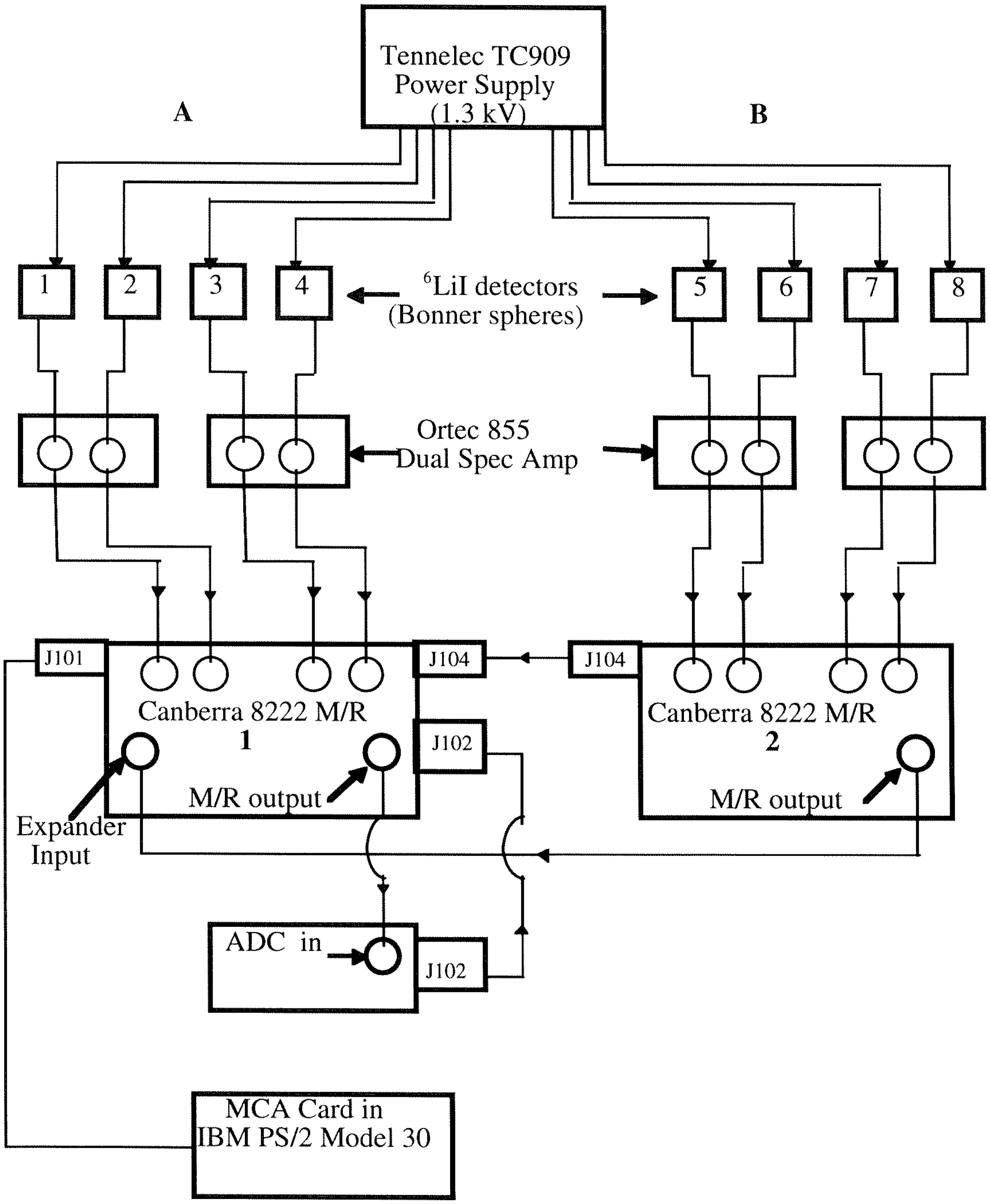

Figure 2. Schematic diagram of Bonner spheres electronics setup.

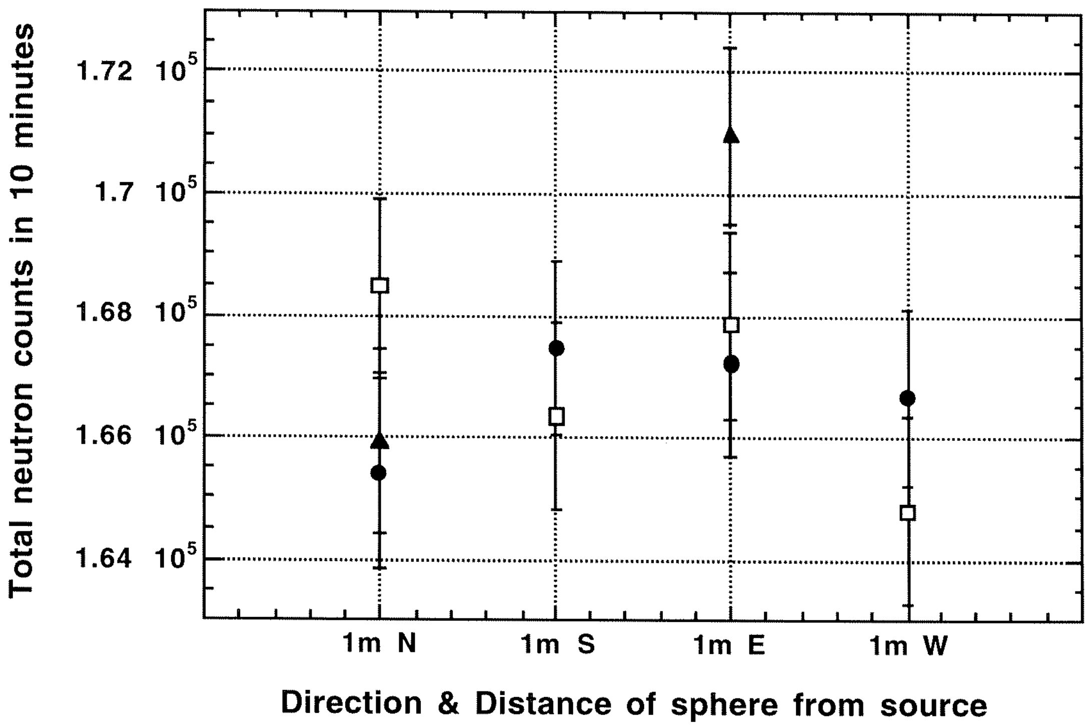

Figure 3a. Test of the uniformity of floor scattering in the RPCF, using the 12.7 cm sphere moved in cardinal directions. The source-detector distance $r_0 = 1$ m.

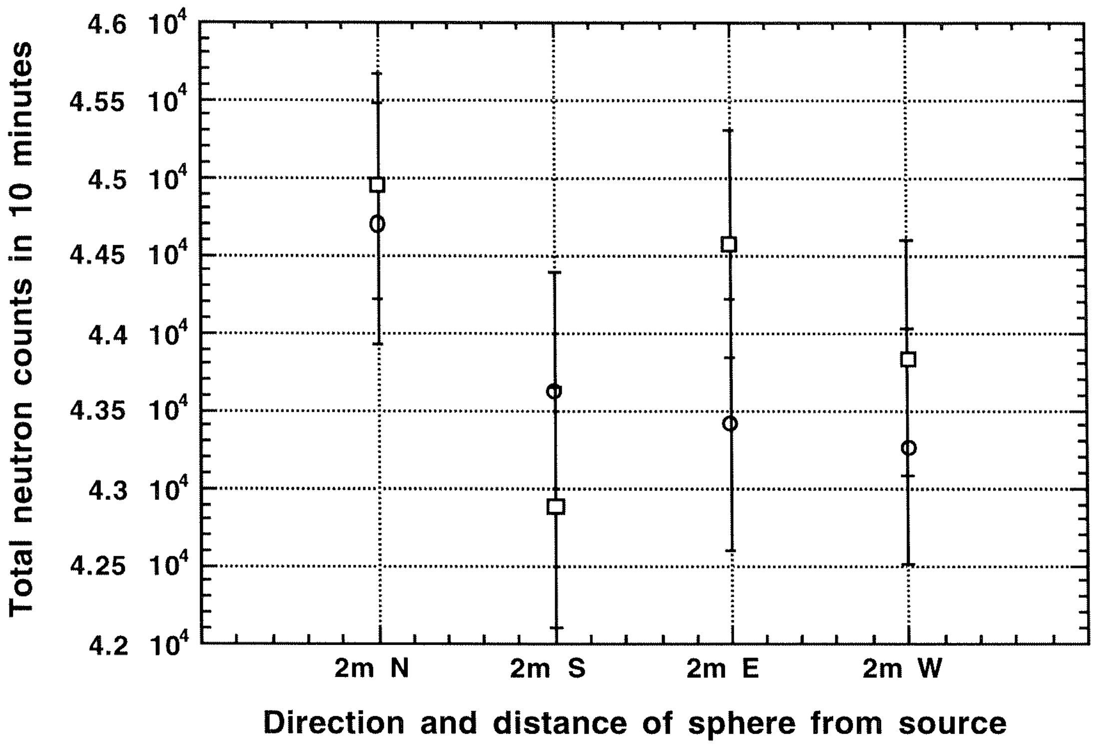

Figure 3b. Test of the uniformity of floor scattering in the RPCF, using the 12.7 cm sphere moved in cardinal directions. The source-detector distance $r_0 = 2$ m.

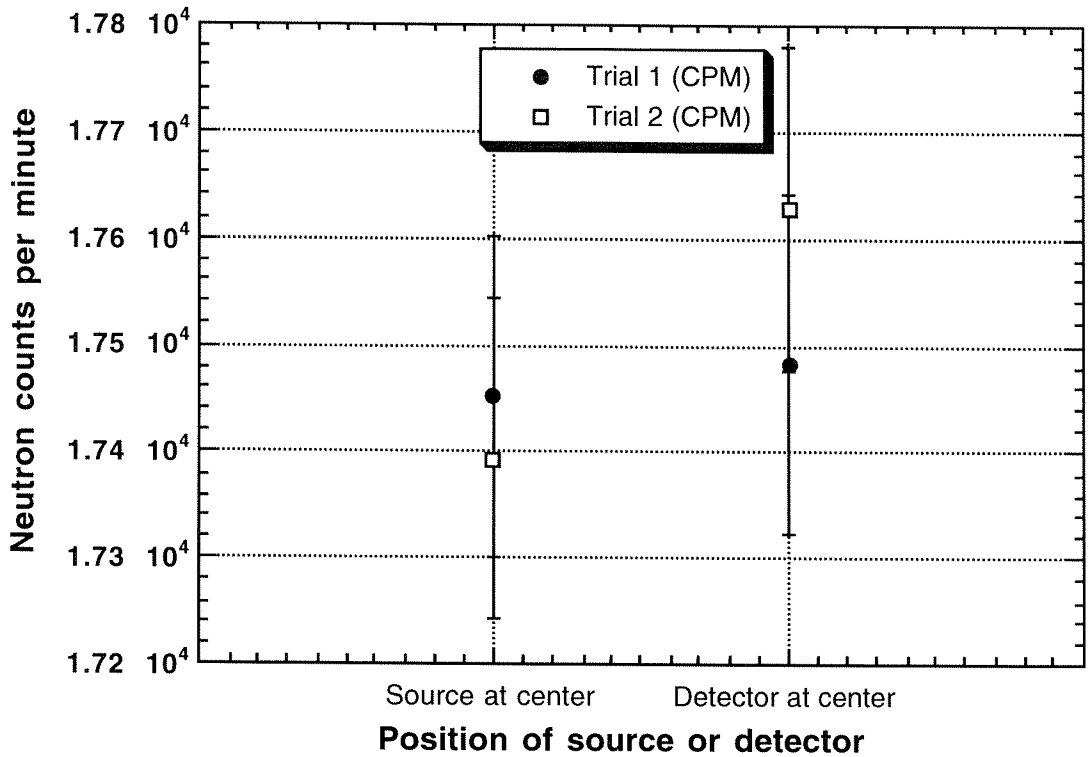

Figure 4a. Test of the uniformity of floor scattering when source and detector are at floor center. The source-detector distance r_0= 1 m.

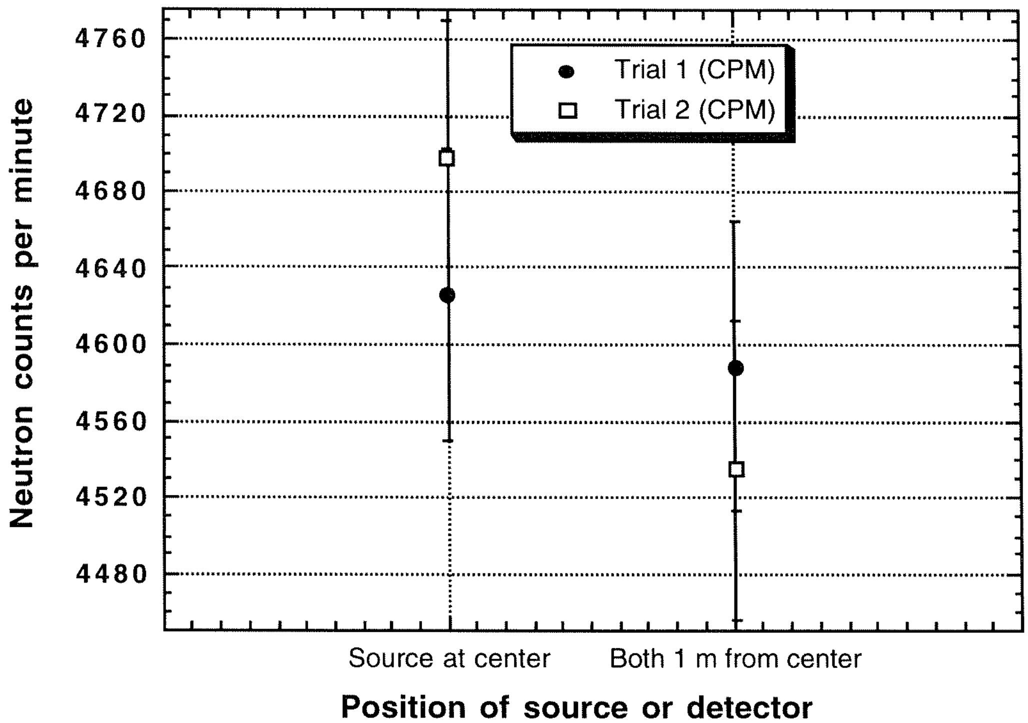

Figure 4b. Test of the uniformity of floor scattering when source and detector are at floor center. The source-detector distance r_0= 2 m.

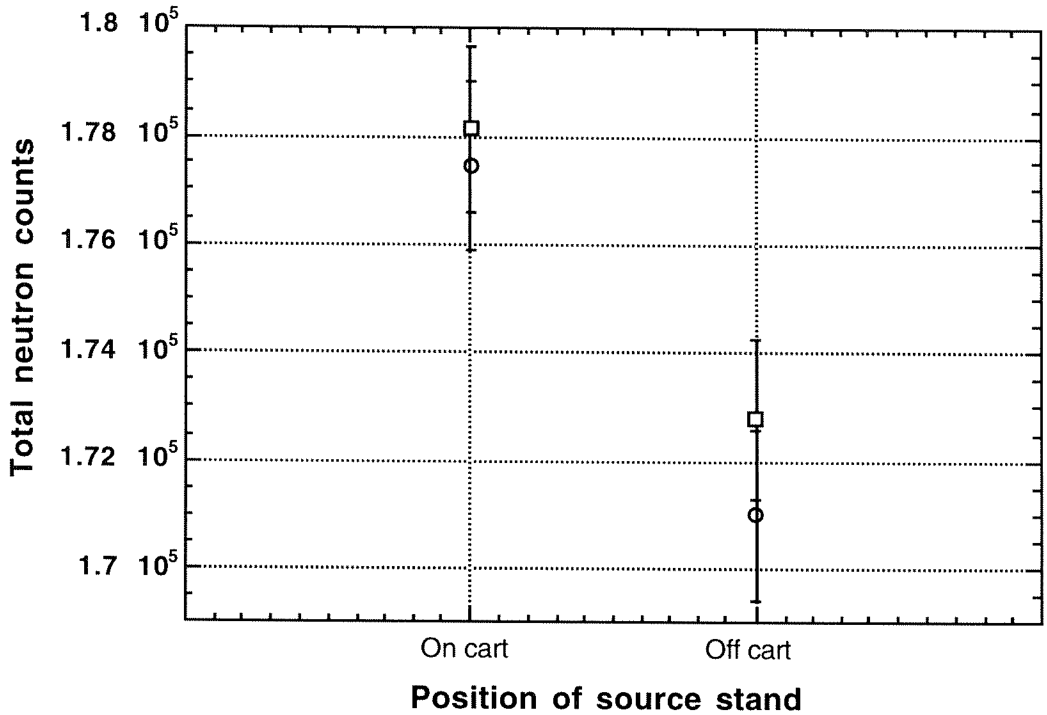

Figure 5a: Determination of the wooden platform's contribution to scattered neutrons. The 12.7 cm sphere was used in two trials. The source-detector distance $r_0 = 1$ m, height = 0.375 m.

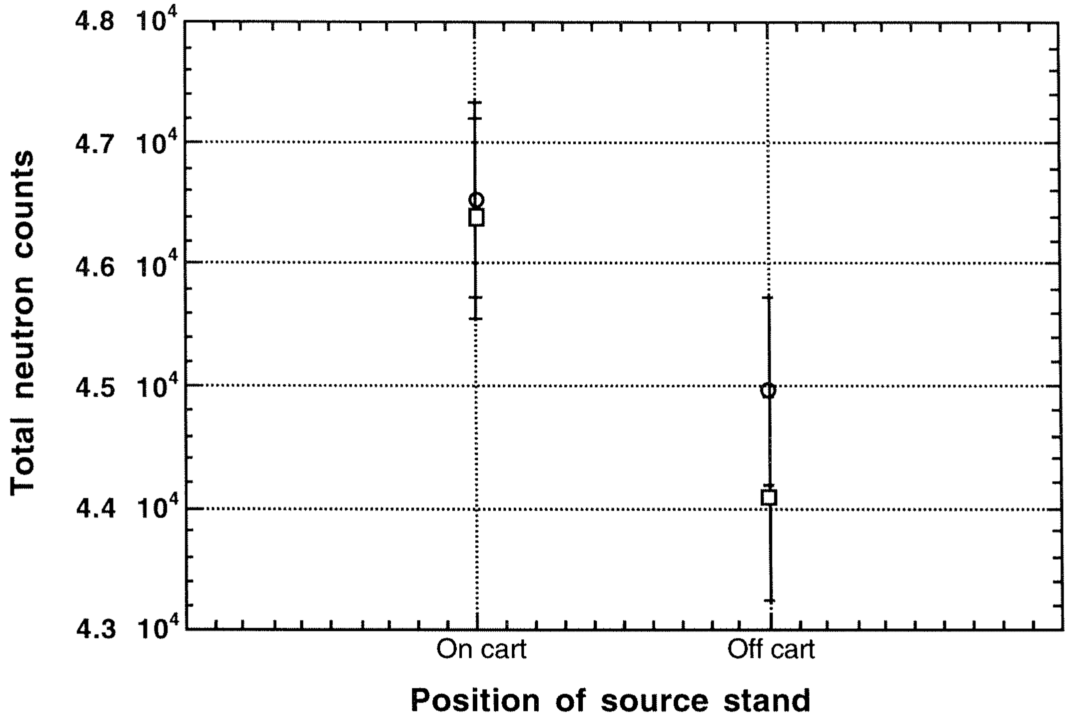

Figure 5b: Determination of the wooden platform's contribution to scattered neutrons. The 12.7 cm sphere was used in two trials. The source-detector distance $r_0 = 2$ m, height = 0.375 m.

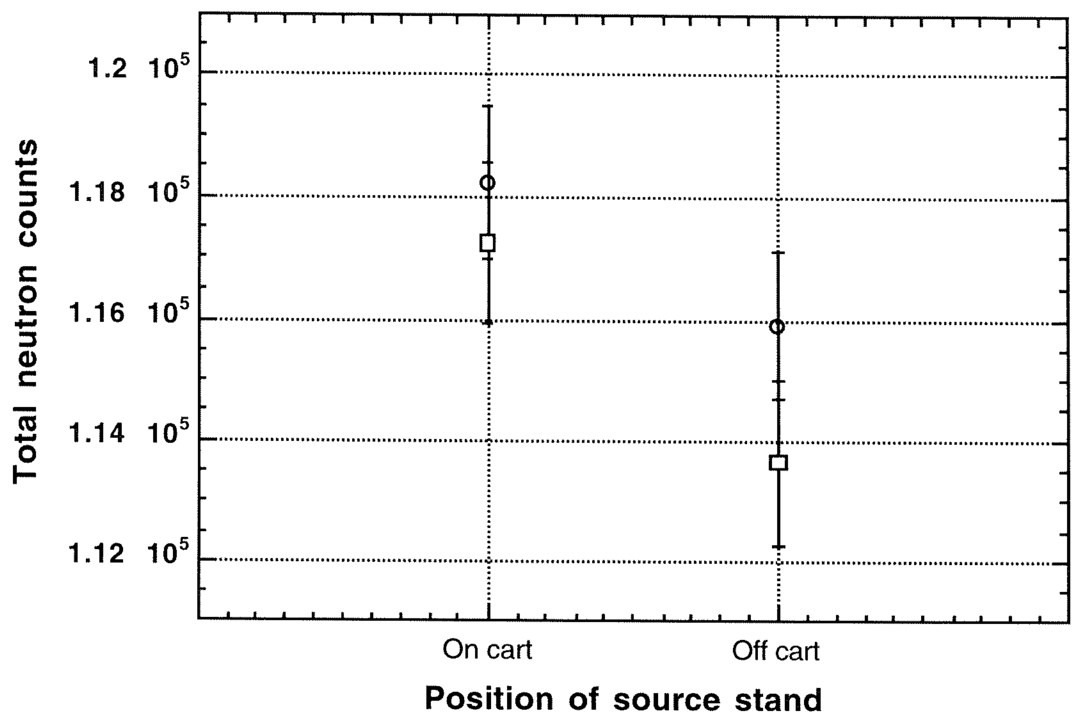

Figure 5c: Determination of the wooden platform's contribution to scattered neutrons. The 12.7 cm sphere was used in two trials. The source-detector distance $r_0 = 1$ m, height = 1.815 m.

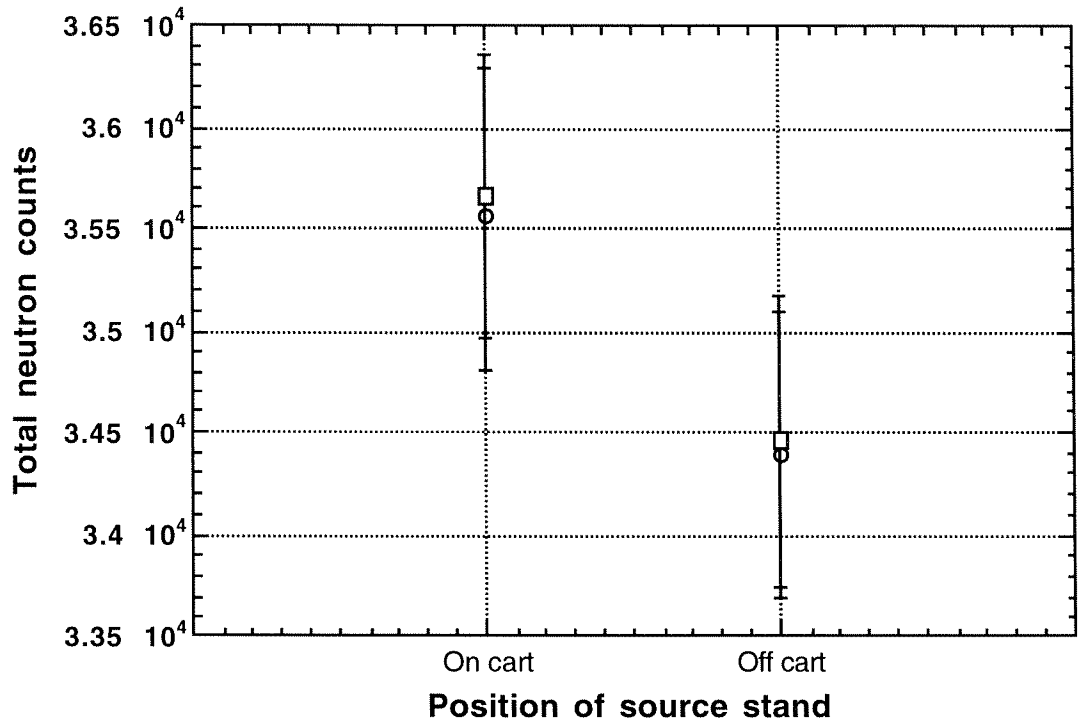

Figure 5d: Determination of the wooden platform's contribution to scattered neutrons. The 12.7 cm sphere was used in two trials. The source-detector distance $r_0 = 2$ m, height = 1.815 m.

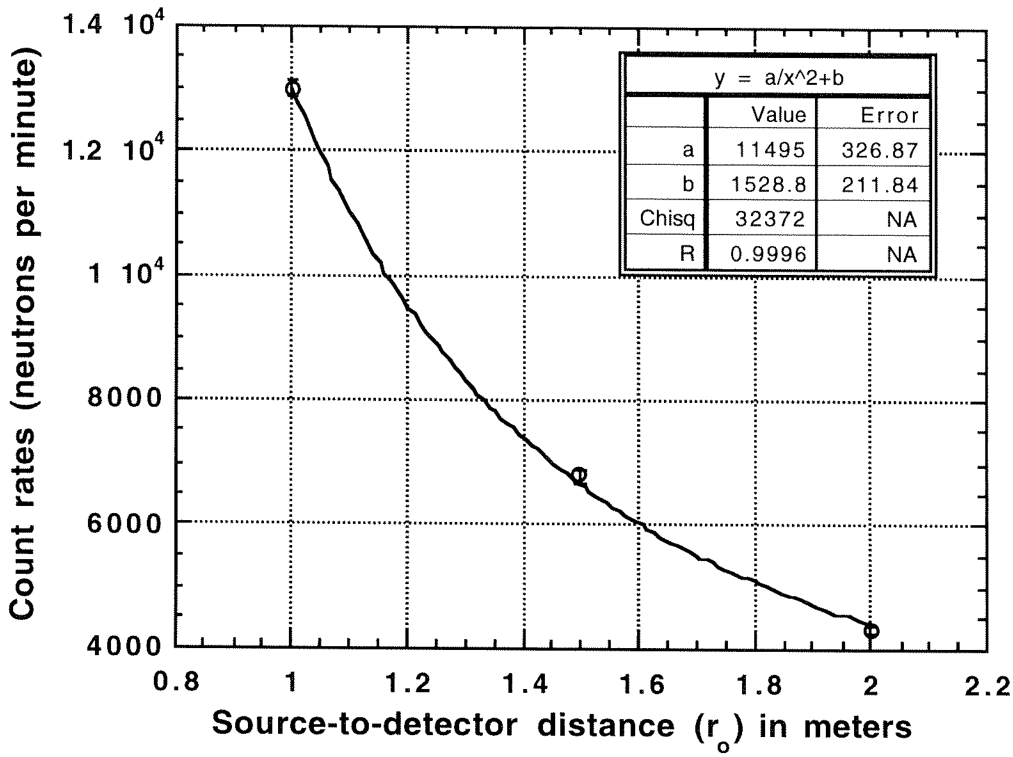

Figure 6. An example of curve-fitting to obtain the direct and scattered neutron fluence portions. This example is for the 12.7 cm diameter sphere at a height of 94.8 cm.

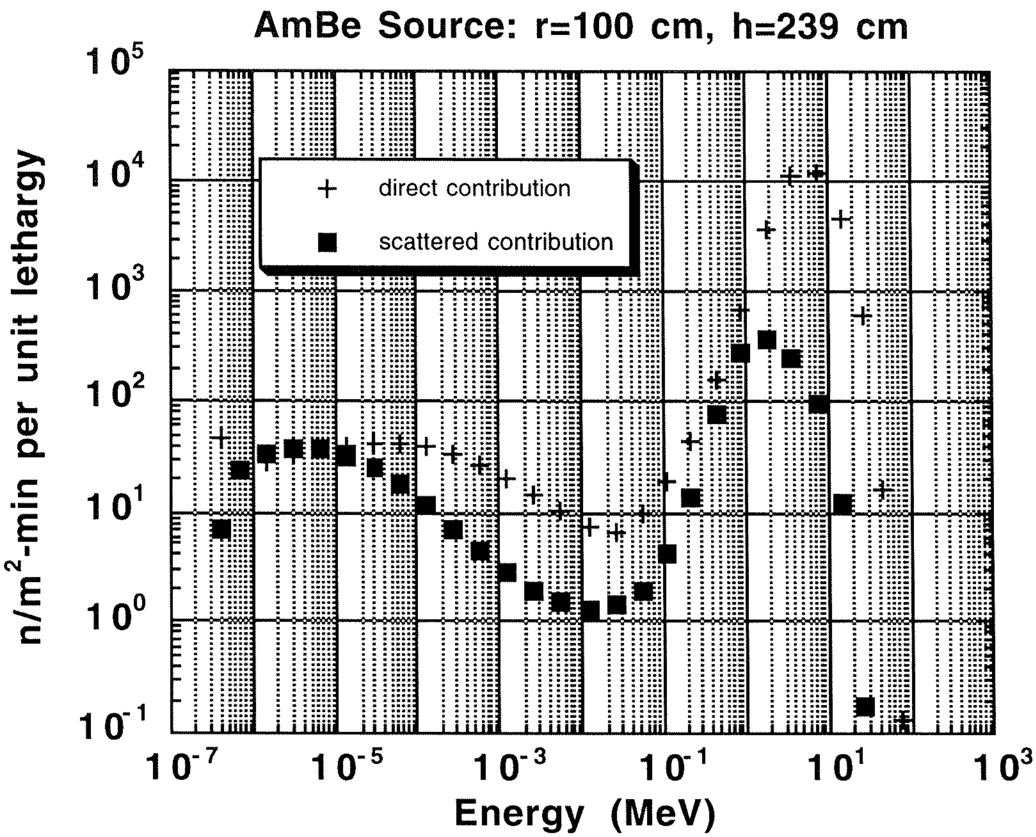

Figure 7. A comparison of direct and scattered neutron spectrum for the AmBe source at a given point.

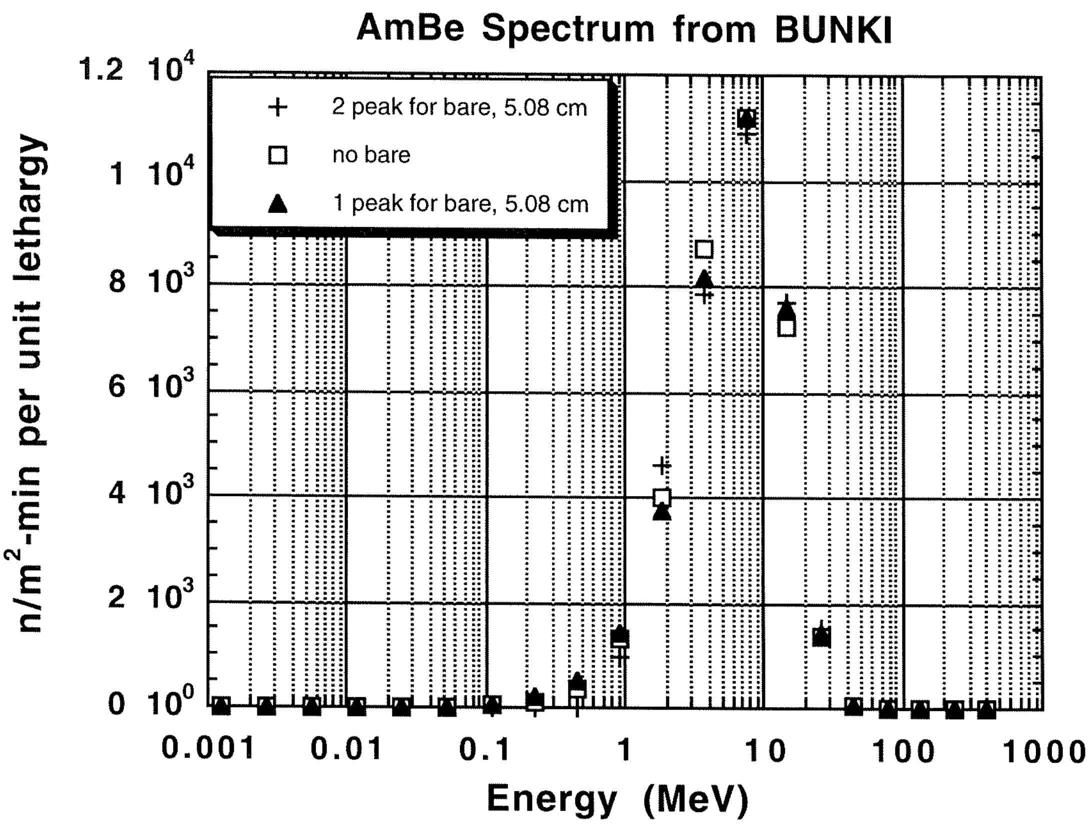

Figure A1. Neutron spectrum of the AmBe source, with and with out the second peak in the bare and 5.08 cm detector data. The spectrum without the bare detector is also shown.